

IS THERE ANY REASON TO CONTINUE RESEARCH EFFORTS IN EROSION-CORROSION?

I. G. Wright

Oak Ridge National Laboratory
Oak Ridge, TN 37831

Abstract

There are many environments in, for instance, power generation processes where components experience mechanical wear superimposed on conditions of aqueous or high-temperature corrosion. Current understanding of the factors considered to determine the response of a material to such conditions involves a large number of independent variables, so that it is not surprising that our ability to select materials for improved performance remains fairly rudimentary. In this paper, an overview is presented of the influence of the major variables used to describe the erosion-corrosion potential of an environment as well as the resistance of a material, and the effectiveness of available predictive approaches based on these is critically examined. The intent of this overview is to highlight areas where the current state of understanding provides a reasonable basis on which future research might be based, and areas where better characterization is needed before phenomenological observations can be described in a mechanistically- (and practically-) useful way.

Introduction

In the first part of this paper a brief overview is provided of the current state of understanding of the factors that influence the erosion behavior of metallic materials, particularly near room temperature, after which an examination is made of how this understanding contributes to our ability to predict the behavior of alloys to resist erosion-corrosion phenomena, where corrosion is limited to high-temperature oxidation in air. The aim of this analysis is to identify what aspects of erosion-corrosion might be worth pursuing in further research with respect to the potential advances to be gained in practical applications where erosion-corrosion is a serious problem.

It is worth considering what are the expected benefits from research on erosion-corrosion. Firstly, it would be hoped that an understanding would be gained of the influence of materials properties on the resistance to erosion-corrosion, and that this would provide an informed basis for materials selection. The types of data required would not only involve means of accurately predicting the rate of materials loss for use in cost-

benefit analyses, for instance, but also information on the mode of materials loss which can provide insight useful for component designers. There is also the hope that research can provide guidelines for alloy modification with the expectation of significantly improving performance in a given environment. Perhaps a more realistic expectation is that research can provide an understanding of the environmental factors of most concern in conditions where erosion and corrosion prevail. Such understanding can be readily translated into practice through modification of process parameters shown to have the greatest influence on erosion-corrosion. Further, such understanding could be used to predict the effects that process changes intended, for instance, to improve process efficiency would have on the erosion-corrosion situation.

Metallic Erosion

The topic of erosion on metallic surfaces by solid particles has given rise to much elegant and insightful research over the past 40 or so years⁽¹⁻⁸⁾. Significant progress has been made in describing and understanding the details of erodent-target interactions and in calculating the energy transferred over a range of circumstances. Nevertheless, in terms of translation of this understanding into practically useful guidelines, it appears that the factors most widely perceived to affect the erosion behavior of materials are mostly descriptors of the erosive environment, while the materials properties most widely regarded as influencing resistance to erosion are hardness, and perhaps toughness. The major environmental factors considered to affect the erosion behavior of metallic materials appear to be: particle velocity; angle of impact; particle size; and the frequency of particle impacts. Three of these are illustrated in Figs. 1-3. Figure 1 demonstrates the important dependence of erosion on particle velocity for a number of materials, ranging from alloys of Mg, Al, Co, and a ferritic chromium steel, to glass, hot-pressed Si₃N₄, and a WC coating. Typically, for metallic materials the erosion rate has been found to be dependent on particle velocity raised to a power of between 2 and 3. Figure 2 shows a well-known dependence of erosion on the incident angle of the eroded particles, in which maximum erosion is experienced for metallic materials (commonly

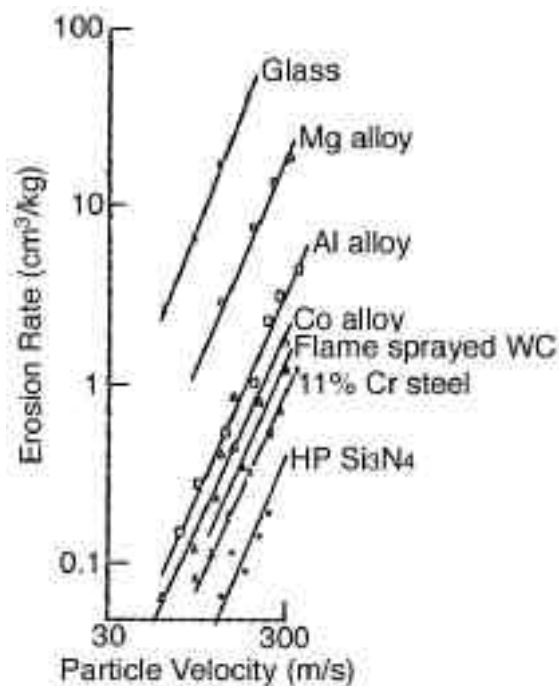


Figure 1. Dependence of erosion loss on particle velocity (room temperature), after Tilly and Sage⁽⁹⁾.

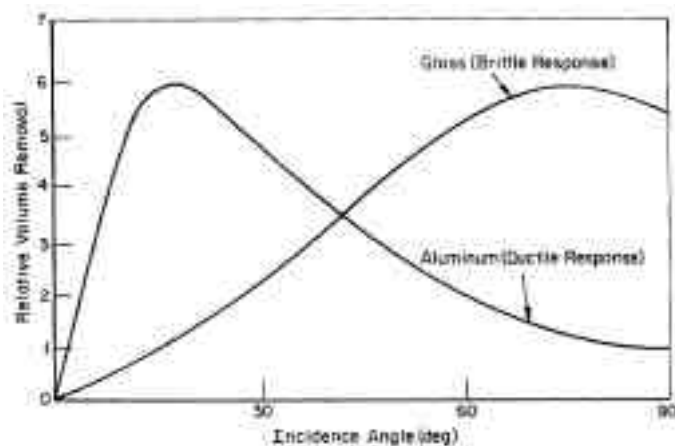


Figure 2. Dependence of erosion loss on incident angle of erodent (room temperature), after Sheldon and Finnie⁽¹⁰⁾.

considered to provide a ductile response to erosion) at an angle of incidence of less than 30° whereas, for materials considered to have a brittle response to erosion (such as ceramics or the ceramic oxide scales formed on oxidizing alloys), maximum erosion loss occurs near 90°. Figure 3 illustrates a finding from several studies that metallic erosion loss increases with increasing erodent particle size up to some limiting size, above which no further increasing damage is found with increasing particle size. This is typically attributed to the fragmentation of larger eroded particles upon impact, or to interference with the

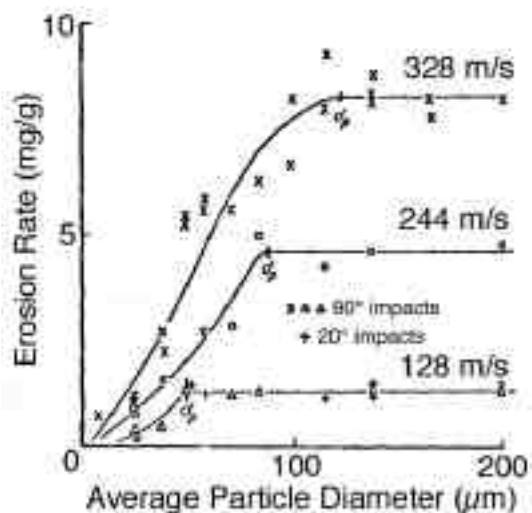


Figure 3. Dependence of metallic erosion loss on erodent particle size (room temperature), after Goodwin, Sage, and Tilly⁽¹¹⁾.

incoming eroded particles by particles rebounding from the target surface, effectively limiting the number of particles capable of striking the surface at full velocity.

The effect on erosion of increasing particle impact frequency (for a given particle size) typically is reported to result in an increase in erosion loss up to some limiting particle loading in the gas, above which interference between impacting and rebounding particles limits further damage. The shape of the eroded particles also affects their ability to remove metal from the target surface. Sharp particles are regarded as being capable of acting as individual cutting tools when impacting at shallow angles of incidence, whereas blunt particles are less effective, at least on initially smooth surfaces, in removing material. For blunt particles the removal process must involve deformation of the surface (by 'plowing') to produce thin raised lips of material, which are then susceptible to being knocked off by subsequent impacts. The properties of the erodent particles also have some influence on their efficiency of material removal. Particles with higher rebound characteristics typically will transfer less of their kinetic energy into the target surface, and particles that are significantly harder than the target surface are usually held to be much more erosive than particles with hardness similar to or less than that of the target.

Note that all the parameters discussed so far involve what can be classed as *process variables*, involving the type of erodent and its presentation to the target surface, and what could readily be changed by modification of the local environment experienced by the component of interest. The major material properties shown to affect erosion behavior of metallic materials are: substrate hardness, as typified by the elegant work of Finnie, et al.,^(1,10) and the microstructure of the target, particularly when the alloy contains a distribution of a second phase such as a carbide. The presence of a distributed particles of a hard second phase in the alloy surface can serve to shield the softer metal on the lee-side of the particles from the erodent,

particularly at shallow angles of erodent incidence. In the limit, a sufficient number or size of second-phase particles in the surface could result in most of the view area of surface area accessible to ('viewed' by) the erodent at a particular incidence angle being covered by these particles, hence the potential for improved erosion resistance.

Attempts have been made to correlate erosion behavior with other target properties such as melting temperature and elastic modulus⁽¹²⁾; adiabatic shear susceptibility⁽¹³⁾; combinations of target specific heat, density, and temperature⁽⁸⁾; or properties that determine the energy absorbed from impacting particles⁽¹⁴⁾. However, although reasonable correlations have been demonstrated, none have supplanted the criterion of hardness in the popular view of erosion.

As an example of the types of dependencies observed, Fig. 4 shows experimental data for a series of pure elements subjected to erosion by solid glass spheres⁽¹⁵⁾. A spherical erodent (with a narrow particle size: average diameter of 14 μm) was chosen so that the impact conditions would be uniform for each particle, and relatively simple to describe. The conditions employed were: particle velocity of 30 m/s (98 ft/s), particle loading in air of 15,000 ppmw, at room temperature. The mean particle size and particle loading were very similar to the conditions found entering the cyclone separator in many coal combustion systems but, while fly ash particles would be silica-rich, their shapes would be randomly angular. Note that for the elements chosen, the hardness of the glass spheres was higher (but not much higher) than all the target materials except Be.

Two features worthy of comment in the experimental data shown are that those for the samples of Pb at 30 and 90° indicate that the erosion behavior was essentially the same at both angles, whereas for Be there was essentially no materials loss measured at 90°. In all the cases illustrated in Fig. 4 there is a suggestion that the erosion rates of the elements decrease with an increase of each of the properties examined. However, if the data points for Pb are ignored, such relationships are not so obvious (except, perhaps, for Vickers hardness). The classic work of Finnie, et al.^(16,17) indicated that the erosion rate of elements of the same crystal structure decreased monotonically with increasing hardness, but that the slopes of the erosion rate-hardness relationships were different for different crystal structures. In the case of the results shown in Fig. 4, Al, Cu, and Ni have the fcc structure, whereas Pb and Fe are bcc, and Be is hcp.

Modeling of Erosion

In addition to the extensive research to characterize erosion behavior, considerable effort has been expended in attempting to model the erosion behavior of metallic materials. A major result is that it has been shown that the behavior resulting from erodent impact at shallow angles can be quite well described by considering the trajectory of individual particles across or into the target surface⁽¹⁾. The major features appear to be 'cutting,' where the leading edge of an angular erodent particle cuts through the surface, and 'plowing,' where the trailing edge of the erodent creates a furrow in the surface resulting in the

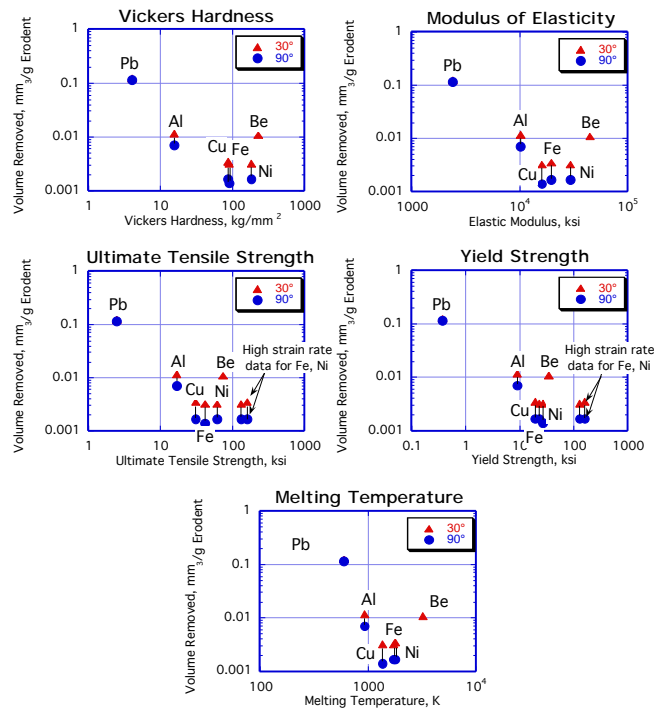


Figure 4. Correlation of erosion rates of metallic elements with materials properties⁽¹³⁾

extrusion of protruding prows of target material that are highly susceptible to removal by subsequent 'cutting' impacts. Similarly, the movement of a blunt particle through the surface will produce lips or protrusions at the end of the crater by plowing. The model developed by Finnie et al.^(16,17) draws an analogy between erosion and cutting wear, in which erosion is assumed to occur by the cutting action of a rigid particle traversing through a ductile target surface; Krushchov, et al.⁽¹⁸⁾; Bitter⁽¹⁹⁾; Neilson and Gilchrist⁽²⁰⁾; and Tilly⁽²¹⁾ also were proponents of this model. According to Finnie's model, the volume of metal removed as a micromachining chip is equal to the volume of the crater swept out by the trajectory of the cutting tip through the surface and the width of the cutting face. Finnie's expression⁽²²⁾ for the volume of material removed (V) for a shallow impact angle $< \tan^{-1}(P/2)$, [where $P = K/(1 + m^2/I)$], is:

$$V = cMv^2/2 \quad [2/K(\sin^2 - 2/P\sin^2)] \quad (1)$$

Whereas, for $> \tan^{-1}(P/2)$,

$$V = cMv^2/2 \quad [\cos^2 (1+m^2/I)^{-1}] \quad (2)$$

where: c is the fraction of particles that actually cut the surface in the manner assumed; M is the total mass of erodent impacting the surface; v is the erodent velocity; θ is the ratio of the vertical distance over which the erodent penetrates the surface to the depth of cut; r is the horizontal component of flow pressure between particle

and surface; m is the mass of an individual erodent particle; I is the mass moment of inertia around its center of gravity; and K is a constant.

For 30° impacts, the appropriate expression is:

$$\text{Erosion rate} = \rho_m (c/2) [\cos^2 (\theta) (1 + mr^2/I)^{-1}] v \quad (3)$$

(where erosion loss is in terms of mass loss/mass impacted); this can be simplified (for $\theta = 30^\circ$) to:

$$\text{Erosion loss (mg/g)} = 7.172 \times 10^{-4} \rho_m / H_v v^2 \quad (4)$$

where: ρ_m is the density of the target (g/cm^3), H_v is the Vickers hardness (kg/m^2) of the target surface, and v is in m/s.

Experimental results have suggested that the velocity exponent of erosion at low angles of impingement is somewhat greater than 2.0 (ranging from 2 to 3), due to a particle size effect⁽¹⁷⁾ and the fragmentation of the erodent particles upon impact⁽²¹⁾. Finnie made a slight revision of the model to account for this observation. In the modified model, the position of the forces acting on the erodent was moved from the particle tip to the center of the contact region between the particle and the surface, so modifying the rotational motion of the particle⁽¹⁷⁾. This resulted in a slight change in the shape of the crater formed, and predicted a velocity exponent that increases with increasing impact angle. Nevertheless, for large particles that do not fragment these explanations would not apply, and a velocity exponent of two would be expected. A limitation of the cutting model is that at angles greater than that corresponding to maximum loss, the erosion loss is underestimated and no material removal is predicted for normal impacts, whereas observations suggest otherwise.

The Cambridge group^(7,13,23) made some pertinent observations of the influence of the actual motion of the erodent particles during erosion on the mechanisms of material removal. Single impacts of angular particles at cutting rake angles were found to displace, rather than remove, a lip or prow of material, whereas plowing impacts displaced material to the sides of the impact crater; detachment of this material only occurred for larger particles above some critical velocity. Hutchings, et al.⁽²⁴⁾ also conducted studies using spherical particles which indicated that the major mode of material removal was from detachment of a fraction of the material displaced to form a lip at the end of the erosion crater. Detachment was associated with the formation of a band of intense shear deformation beneath the surface near the lip. For these cases, a velocity exponent of 2.9 (for mass loss) was measured. These workers suggested that contributions to erosion that do not involve plowing impacts are relatively insensitive to velocity, and that in those cases the velocity exponent is probably less than 2.4. Overall, it appears that the actual processes of material loss by erosion at shallow impact angles may be numerous, with one or several dominating under given conditions of erodent shape, impact velocity, and erodent and target mechanical properties.

Most of the attempts to model erosion at or near a normal

incident angle are based on the assumption that the target surface eventually fatigues, which provides the mechanisms whereby undulations can develop in the eroded surface and so render it susceptible to material removal. Very diligent attempts have been made to provide mathematical descriptions of the response of metal surfaces to normal impacts. Notable among these are those of Hutchings⁽²³⁾, Mamoun⁽²⁵⁾, and Sundararajan and Shewman⁽²⁶⁾, which invoke the materials parameters that control strain hardening, fatigue, and local plastic flow. One difficulty experienced by all of the normal impact models is in defining a criterion for initiation of material loss. Delamination of work-hardened and fatigued surface layers is one much-cited mechanism, which presumably results from local plastic flow of the target surface upon impact, with eventual crack initiation and propagation to separate these layers from the surface. Deformation mechanisms, including micro-slip leading to local heating and adiabatic shear, also have been invoked as a means of displacing surface material to form prows of material that are susceptible to deformation and removal by subsequent impacts.

Using as examples two of the more tractable models for normal impact, the relationship derived by Hutchings⁽²³⁾ can be expressed as:

$$\text{Erosion Loss} = 0.033(a \rho_m^{0.5} V^3) / (c_s^2 P^{1.5}) \quad (5)$$

where: a is some fraction of the volume of the indentation; ρ_m is the density of the target material; c_s is the shear strength of the target surface; V is the particle velocity at impact; c_s is the critical strain of the target surface, and P can be related to the quasi-static indentation hardness of the substrate.

In contrast, the relationship of Sundararajan and Shewman⁽²⁶⁾, which involves parameters that are intended to include thermal properties of the target, can be simplified to:

$$\text{Erosion Loss} = 6.5 \times 10^{-3} (V^{2.5} \rho_b^{0.25}) / (C_p T_m^{0.75} H_s^{0.25}) \quad (6)$$

where: ρ_b is the density of the target; C_p is the target specific heat; T_m is a target melting temperature, and H_s is a substrate hardness.

The experimental conditions and relevant properties of the elements from the erosion tests described above⁽¹⁵⁾ were used to calculate the erosion rates predicted by these relationships. The resulting predictions for the 30° impact conditions are plotted against the experimental data in Figs. 5(a) and (b).

In these figures the two sets of data points shown for each element represent the extremes of erosion rate derived from the data using: (a) the steady-state erosion rate derived from the slope of the erosion loss versus time curve, shown by the open symbols, and (b) the erosion rate derived by simply dividing the total mass loss of the specimen by the total erodent impacting its surface, as indicated by the solid symbols. Both of Finnie's relationships were tested in this way. Note also that the data for Pb were omitted, since this element exhibited essentially no resistance to erosion. As might have been expected, since Finnie's model is based on the assumption of individual erodents

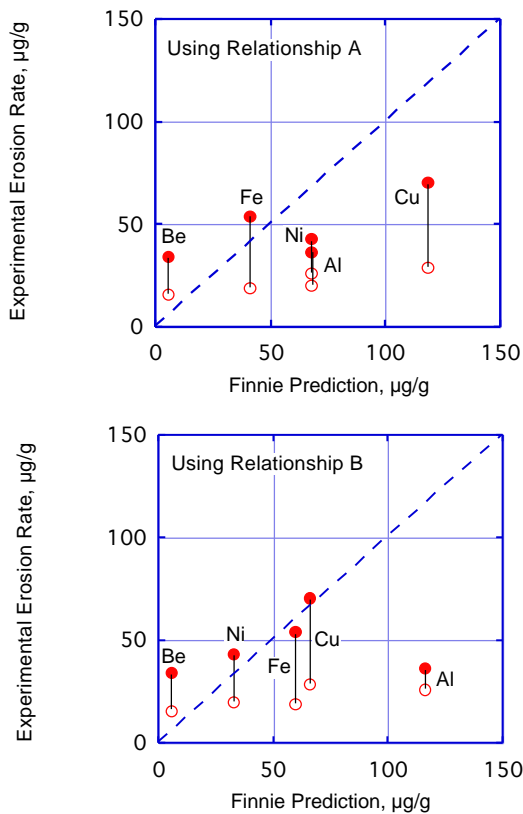


Figure 5. Predicted erosion rates from 30° impacts using (a) Finnie relationship A (eqn. 4); (b) Finnie relationship B(modification to give variable velocity exponent); the dotted line indicates a perfect correlation.

acting as cutting tools, the metal loss for Cu, Al, and Ni (fcc structures) were over-predicted, while the material loss from Be was under-predicted. Finnie's relationship (B) was a modification of (A), taking into account the rotation of the individual erodents (or cutting tools) as they passed through the target surface^(2,17). This resulted in displacement of material from the sides of the cutting groove and its subsequent removal by cutting from later impacts, but again over-predicted the loss from Al, Cu, and Fe (when considering the data derived from the slopes of the erosion curves), and again under-predicted the loss from Be.

The performance of the Hutchings and Sundararajan and Shewman models is indicated in Figs. 6 and 7. Curiously, the Hutchings model under-predicted the material loss from all the elements except Cu (for which the two alternative experimental data points exhibited wide scatter) whereas the Sundararajan and Shewman model over-predicted the loss from all materials.

Erosion-Corrosion

When corrosion in the form of high-temperature oxidation is combined with an erosive environment, two major new variables must be taken into account: temperature and

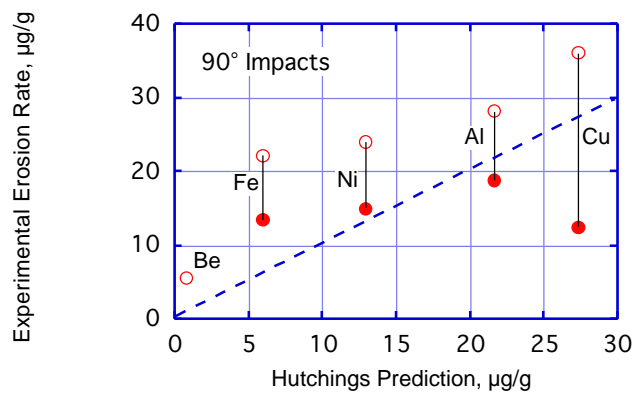


Figure 6. Predicted erosion rates from 90° impacts using Hutchings' relationship⁽²³⁾. The dotted line indicates a perfect correlation.

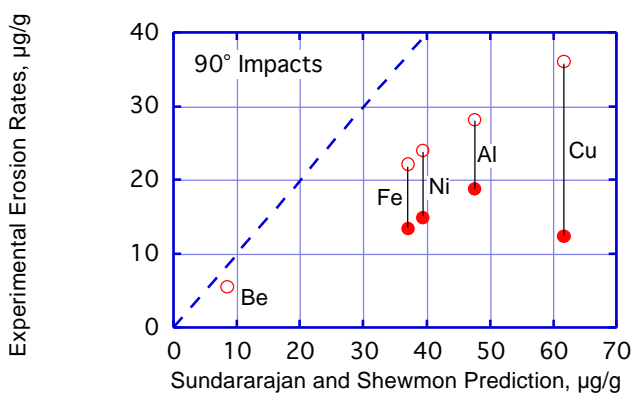


Figure 7. Predicted erosion rates from 90° impacts using Sundararajan and Shewman's relationship⁽²⁶⁾. The dotted line indicates a perfect correlation.

frequency of impacts. The mechanical properties expected to control the erosion response of metals are significantly changed by temperature: properties such as hardness and toughness are affected in ways that would be expected intuitively to decrease and increase resistance to erosion, respectively. Increased temperature also promotes the development on the target surface of oxide scales. Such scales typically have a much higher hardness than the substrate so that, if they remain adherent to the surface, they would be expected to modify its response to erodent impacts. Further, the rate of surface scale growth is proportional to temperature (T), typically represented as:

$$\text{Scale thickness, } S = Ae^{-Q/RT} t \quad (7)$$

where: Q is the activation energy for the oxidation process; R is the universal gas constant; and t is time.

With increasing temperature the alloy substrate will tend to become weaker, while growing a surface ceramic layer at an increasing rate. When a surface oxide is present, its interaction with impinging erodent particles will modify the erosion

response of the target surface. Erodent impacts on the oxide scale may damage it, or cause it to spall, resulting in a localized increase in oxidation rate that depends on the extent to which the effective thickness (length of diffusion path) of the scale was decreased. In this scenario, the frequency of erosive impacts capable of damaging or removing the scale also becomes an important variable. In room-temperature erosion the amount of material removed is, in most cases, proportional to the total number of impacts and is not affected by the frequency of impacts unless the particle loading becomes sufficiently high that interference occurs among impacting and rebounding erodents. In contrast, when erodents impact an oxide-covered surface, any damage to the oxide scale will result in an increase in the oxidation rate in the damaged region, and the extent of the increase will depend on whether oxide is cracked, chipped, or physically removed.

Figure 8 illustrates the mass loss curves for the erosion-oxidation of a range of practical alloys chosen to have a large variation in substrate hardness while having inherently low oxidation rates⁽²⁷⁾. The conditions were chosen to simulate those in the gas stream entering the first cyclone separators in coal combustion systems such as fluidized-bed combustors (the one major difference being the use of alumina particles as erodent for practical reasons; in reality the erodent would be coal fly ash, consisting largely of alumino-silicates). The alloy compositions are listed in Table I along with their hardnesses at room temperature and at 871°C (1600°F). All these alloys are capable of forming a protective oxide scale and have microstructures that range from very high volume fractions of hard carbide particles (Stellite alloys 1, 6B, and 12), to oxide dispersion-strengthened substrates (Inconel 754 and Haynes 8077), to simple solid solution-strengthened structures (type 446).

The responses of the alloys at an erodent velocity of 19 m/s (63 ft/s), in terms of specimen mass change as a function of the mass of impacting erodent, are summarized in Fig. 8(a). Under these conditions, very little mass change was recorded for any of the alloys. The exposure time in these tests to the hot gas was 109 hours, and the mass changes observed were essentially the same as those observed for oxidation alone in an equivalent time⁽²⁷⁾. Figure 8(b) shows the response of the same alloys to impacts at 52 m/s (170 ft/s) at 30°. In this case the total exposure time to hot gas was approximately 31 hours, and all the alloys exhibited mass loss at a linear rate. In all cases the rate of loss was more than an order of magnitude faster than mass losses observed for oxidation alone in a high-velocity gas stream at the same temperature. The responses of the alloys appeared to fall into three groups, with the group showing the lowest rate of loss and that showing the fastest rate of loss being composed of alloys designed to form adherent protective scales, while the middle group comprised the Stellite family of alloys which had varying contents of carbides, hence a wide range of hardness. One conclusion that may be drawn from these data is that there was no obvious influence of substrate hardness on the response of the alloys to erosion-oxidation. There also is the suggestion of a threshold in particle kinetic energy such that below this threshold the damage is apparently confined to the oxide scale,

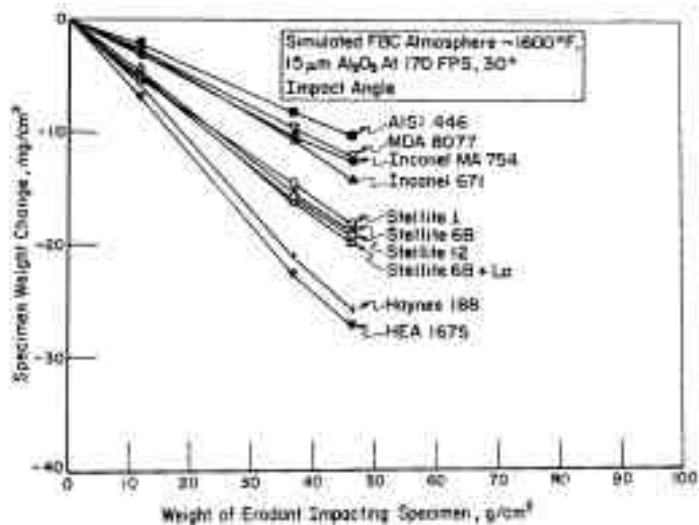


Figure 8. Erosion-oxidation kinetics for a range of practical alloys at 871°C in a simulated FBC flue gas containing 15,000 ppm 15 μ m alumina particles as erodent impacting at 30° at (a) 19 m/s; and (b) 52 m/s; from Wright, Nagarajan, and Herchenroeder⁽²⁷⁾.

since as in Fig. 8(a) there is negligible contribution of the erodent to the overall mass change, whereas at kinetic energies above the threshold the erodent impacts presumably penetrate the oxide, damage and remove it so that sustained linear rates of loss such as shown in Fig. 8(b) are observed. Presumably at particle kinetic energies in the vicinity of the threshold value, the oxide scales will be damaged and possibly partially removed such that the rate of oxidation would be accelerated above that experienced in the absence of erosion, so that either increased mass gain or some degree of mass loss would be reported

Table I. Alloy Compositions (weight percent)

Alloy	Fe	Ni	Co	Cr	Al	Si	W	C	Other	DPH	
										RT	871°C
AISI 446 ^a	Bal	0.26	—	24.00	—	0.44	—	0.15	0.138N	192	19
Inconel 671 ^{a,b}	—	Bal	—	48.0	—	—	—	0.05	0.35Ti	215	63
InconelMA754 ^{a,b}	—	Bal	—	20.00	0.6	—	—	—	0.6Y ₂ O ₃ , 1.2Ti	273	84
Haynes 8077 ^{a,c}	—	Bal	—	16.00	4.0	—	—	—	1.8Y ₂ O ₃	372	84
Haynes 188 ^a	1.48	22.32	Bal	22.39	—	0.442	14.17	0.10	0.035La	244	114
Haynes 1675 ^c	0.15	19.59	Bal	15.27	4.17	0.27	7.50	0.22	0.03Y, 0.55Ta	231	84
Haynes 1775 ^c	2.96	2.61	Bal	31.03	0.13	0.46	3.75	0.84	0.18Mo, 0.03La	372	92
Stellite No. 1 ^d	0.65	0.98	Bal	32.00	—	1.10	12.0	2.33	0.18Mo	638	126
Stellite No. 6B ^d	2.52	2.78	Bal	30.70	—	0.49	4.13	1.06	1.40Mo	341	99
Stellite No. 12 ^d	1.90	1.03	Bal	30.07	—	1.31	8.70	1.43	0.19Mo	497	126

a: nominal composition

b: Special Metals-Huntington Alloys, Huntington, West Virginia

c: Haynes developmental alloy

d: Haynes Stellite, Kokomo, Indiana

depending on the extent to which the oxide was damaged or removed.

Modeling of Erosion-Corrosion

In order to begin to model the erosion-corrosion processes, a number of assumptions must be made concerning the interaction of the erodent particles with the surface. For the case where an alloy has a continuous, adherent oxide scale, the damage inflicted by an impacting erodent particle can be considered to depend on the particle kinetic energy (particle size and velocity) as well as its angle of incidence. Figure 9 is a schematic representation of the extremes of the scenarios discussed for Fig. 8, for an erodent particle with low kinetic energy (Fig. 9a) striking the surface of an alloy that grows an oxide scale at a slow rate (inherently oxidation resistant, or at a low temperature)⁽²⁸⁾. In Fig. 9a it is postulated that, where the result of the erodent impact is confined to the surface oxide layer and results in damaging the layer by chipping and local spallation, the overall result of adding erosion to this oxidizing environment is to accelerate the regrowth of surface oxide in the areas where it has been thinned by damage, followed by the resumption of protective oxidation behavior. The overall change in the surface scale morphology for a low flux of erodent particles would be the appearance of isolated nodules of thickened oxide as well as areas of damage that have been healed (Fig. 9aiiia). In contrast, for a high erodent particle flux it would be expected that the whole of the oxide scale would have been thickened as a result of continuous loss from its outer surface, followed by an acceleration of the oxidation rate. (Fig. 9aiib)

In a case where the same oxidizing surface is impacted by erodent particles with sufficient kinetic energy to penetrate the oxide film and deform the metal substrate (Fig. 9b), it then becomes possible that not only is oxide removed locally from the surface resulting in rapid re-oxidation of these areas, but also areas of deformed metal may also be lost by direct cutting by subsequent impacts. The resulting surface morphology would initially show significant local thickening of the oxide in the

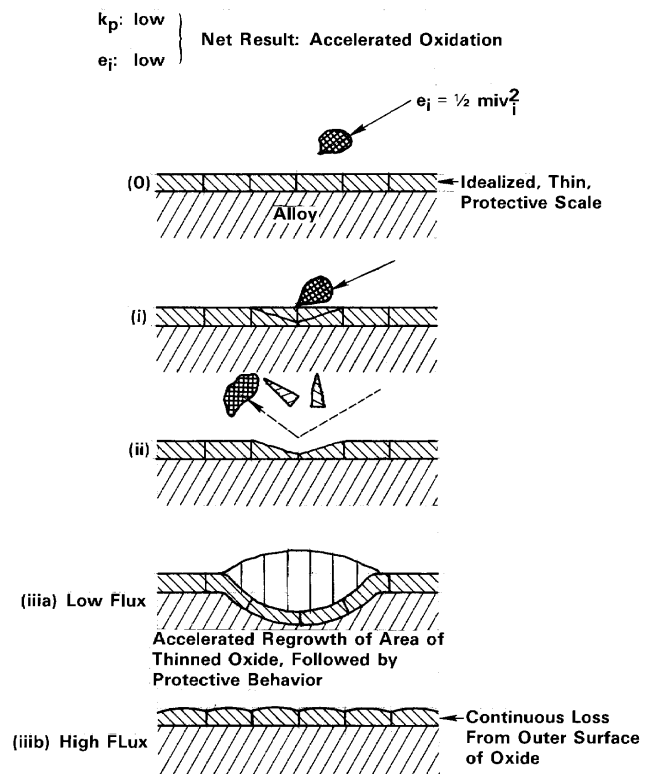


Figure 9a. Schematic representation of scenarios corresponding to slow oxidation rate and low erodent kinetic energy, leading to accelerated oxidation (Wright, Nagarajan, and Stringer⁽²⁸⁾).

impacted areas. For alloys designed to form protective oxide scales, a change to very rapid oxidation can occur when the alloy reservoir of the protective scale-forming element becomes depleted below some critical level. Such depletion is accelerated by constant oxide removal by erodent impact and spallation. As a result, conditions where a protective oxide scale

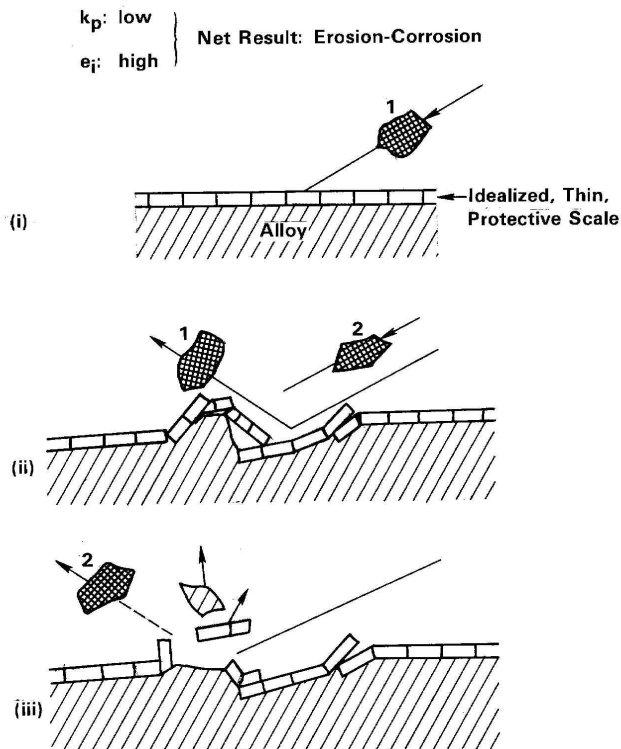


Figure 9b. Schematic representation of scenarios corresponding to slow oxidation rate and high erodent kinetic energy, leading to erosion-oxidation (Wright, Nagarajan, and Stringer⁽²⁸⁾).

can no longer be maintained will be reached more quickly with an increased number (flux) of erodent impacts, and breakaway oxidation will ensue with the target surface becoming covered by a thick, rapidly-growing oxide.

Despite the complex series of events occurring on the surface of a material exposed to the combined action of oxidation and erosion, and notwithstanding the large number of variables involved, several approaches have been suggested for modeling erosion-oxidation processes. A relatively simple approach⁽²⁹⁻³¹⁾ was based on the scenarios just discussed: erosion impacts are assumed to remove the protective oxide, which results in regrowth of the oxide in the areas affected at a rate that depends on the thickness of the oxide remaining at that location. Essentially, the oxidation clock is reset to the time on the assumed parabolic oxidation curve corresponding to the thickness of the remaining oxide. This is illustrated in Fig. 10, which shows the oxide thickness-time curve for a particular area of surface which is subject to particle impacts at frequency F_3 (corresponding to time T_{F_3}), where each impact is assumed to remove the oxide back to the bare metal. The result as shown in Fig. 10 is that the oxidation rate curve is changed from parabolic to essentially linear. Figure 11 shows schematically the expected effects of changing the frequency of impacts [i.e., changing the thickness of oxide grown between impacts (Fig.

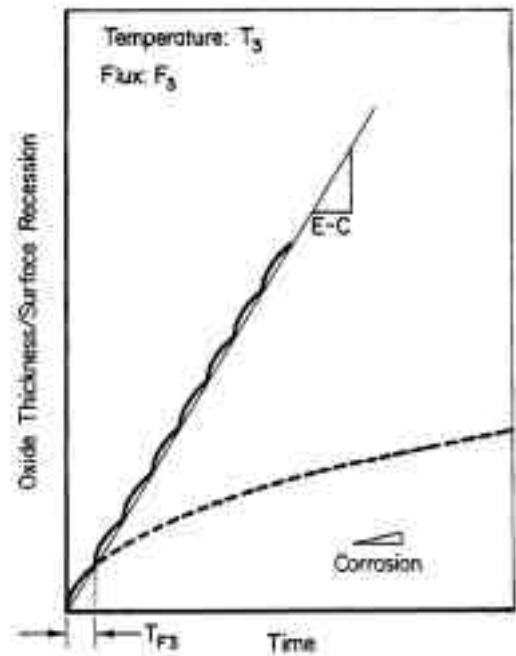


Figure 10. Schematic representation of erosion-oxidation kinetics at temperature T_3 and an erodent flux of F_3 , where the time between successive erodent impacts (scale spallation events) is t_{F_3} (from Sethi and Wright⁽²⁹⁾).

11a)], and the effect of increasing oxidation temperature, [i.e., increasing the oxidation rate at a given particle flux (Fig. 11b)]. As the time between impacts is reduced at a given temperature by increasing the particle flux, the overall linear oxidation rate increases. Similarly, increasing the oxide thickness that can form between successive impacts (by increasing the oxidation temperature) leads to an increase in the net rate of thickening of the oxide scale. Translation of these ideas into a mathematical description of the process involves the assumptions, that:

- the oxide grows by a parabolic rate law, and a uniform, single-phase oxide is formed;
- no direct removal of metal occurs;
- the mechanical properties of the alloy substrate are essentially irrelevant;
- the erosion component consists of spatially-random impacts at a frequency F , hence, the time available for oxide regrowth in a given area is T_F ; and
- each impact results in oxide spallation.

Obviously, such assumptions are only valid for particle kinetic energies between certain limits. Further major assumptions required concern (i) the extent of oxide thickness removed per impact, and (ii) the surface area over which oxide is lost from each erodent impact. The thickness lost may range from only an outer part of the oxide, or the full oxide thickness back

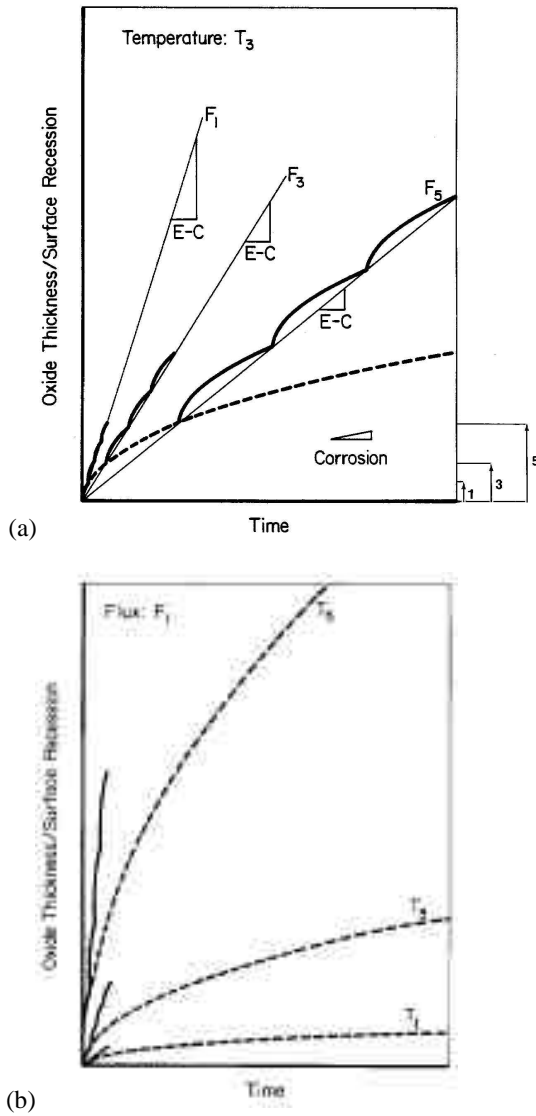


Figure 11. Schematic representation of effect on erosion-oxidation kinetics of (a) changing erodent flux at temperature T_3 (flux $F_1 = 4 \times F_3$ and $16 \times F_5$), and (b) changing oxidation temperature at erodent flux F_1 (parabolic rate constant k_p at $T_5 = 4 \times k_p$ at T_3 , and $16 \times k_p$ at T_1)⁽³⁰⁾.

to the alloy surface, and the extent of removal may not be uniform for any given impact. Such considerations require either accurate measurements of actual, reproducible behavior, or an approach for describing the process using statistical means. In the model described below, it was assumed that the target surface was planar, of infinite size, and that oxidation occurred at a surface temperature of T ; further, a uniform thickness of oxide was removed over an area directly proportional to the projected area beneath each impinging erodent particle. In the absence of useful measurements, these factors were represented by an "erosion footprint," shown schematically in Fig. 12.

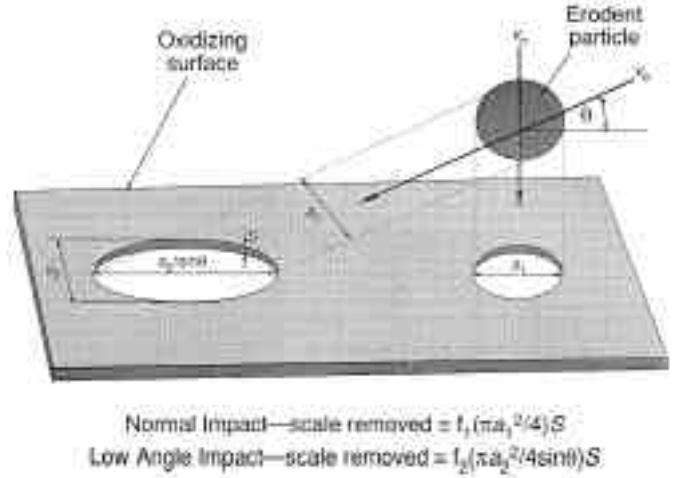


Figure 12. Schematic representation of 'erosion footprints' for an erodent particle striking the target surface at shallow and normal angles; a_1 and a_2 are the projected erodent particle diameters at the shallow () and normal angles of incidence, respectively⁽³²⁾

Using this approach, the oxide removed for a normal impact is given by:

$$\text{Loss} = \text{fctn.}(a_1^2 / 4)S \quad (8)$$

where a_1 is the mean area of the erodent particle projected onto the target surface and S is the oxide thickness removed. For low-angle impacts the relationship becomes:

$$\text{Loss} = \text{fctn.}[a_2^2 / (4\sin^2 \theta)]S \quad (9)$$

where: a_2 is the effective diameter of the erodent particle (which may or may not be the same as a_1), and θ is the angle of erodent incidence. The oxide thickness (S) is given by eqtn. 7.

Markworth⁽³³⁾ suggested that the kinetics of the oxidation-erosion process could be modeled using a deterministic description of the oxidation process (eqtn. 7), while treating the erosion process stochastically. The resulting expression for the coupled oxidation-erosion kinetics, in which the change in oxide thickness is due to random impacts (assuming that the oxide is completely removed by each impact), is:

$$\langle S \rangle = nk / (F a_i^2)^n \quad (n, F a_i^2 t) \quad (10)$$

where: k and n are oxidation mechanism-dependent parameters (i.e., $S = kt^n$); F is the erodent flux; t is time; a_i is the diameter of the erosion footprint; and γ is the incomplete gamma function.

The overall mass change (M_t) is then given by:

$$M_t = (1-f_m)\rho_0 \langle S \rangle - f_m F a_i^2 \rho_0 \langle S \rangle dt \quad (11)$$

where: f_m is the mass fraction of oxide associated with the metallic constituent, and ρ_0 is density of the oxide.

By inspection it can be seen that, as t tends toward zero, the mass change per unit area is positive whereas, as t tends towards infinity, a constant negative mass change results. Figures 13a-c illustrate the trends predicted by such a model and show the

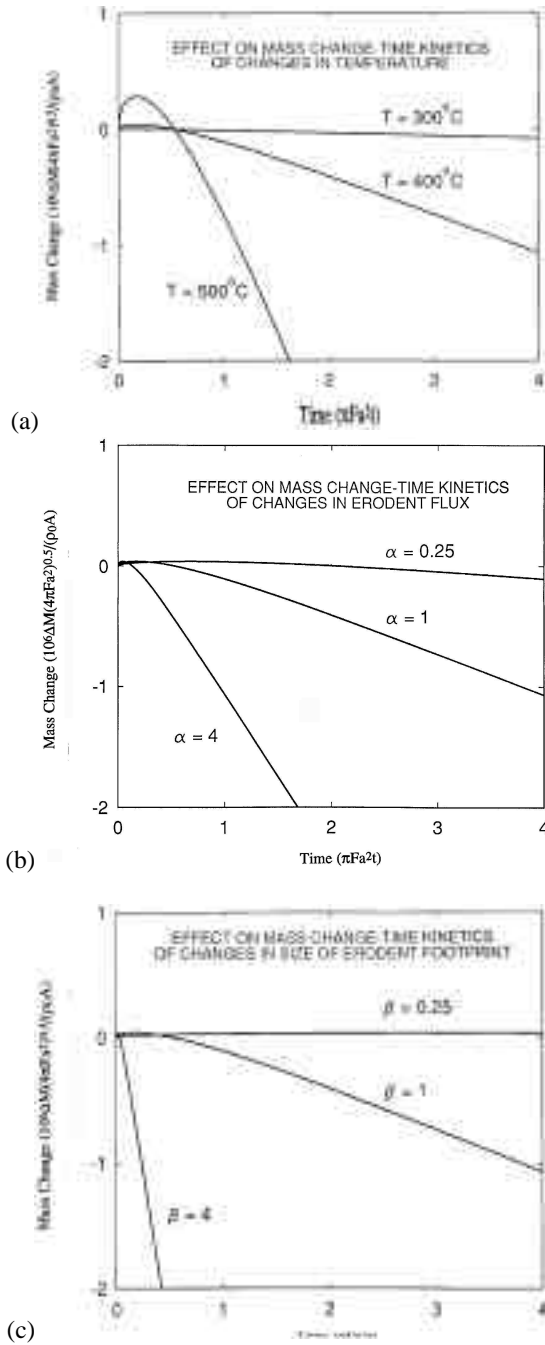


Figure 13. Predictions of variation in mass loss with time as a function of changes in a single variable: (a) temperature; (b) particle flux, where α is the multiplier on flux; and (c) size of erodent footprint, where β is the multiplier on footprint size⁽³⁴⁾.

effects of changing single variables on the mass change-time curves, such as temperature (Fig. 13a), particle flux (Fig 13b), or the size of erodent footprint (Fig 13c). All of the trends shown are quite consistent with those anticipated intuitively, as well as those observed from experimental work. Nevertheless, such results are useful only for providing information on trends since, apart from a value for k_p , it is not possible to independently vary target and erodent property parameters since these are bundled together in the 'erodent footprint.' Presumably, data required to quantify erosion footprints would require very detailed characterization for each specific alloy and erodent combination; it is not known at this point whether all the required parameters are, in fact, quantifiable. As a result, while attempts to quantify and model the response to erosion-oxidation attack of alloys remains a noble goal, the attainment of quantitative results for even the simple case discussed here will likely require the development of cumbersome relationships and large amounts of experimental data, or an extension of the type of statistical treatment illustrated above to describe the 'erosion footprint.' Nicholls and Stephenson⁽³⁵⁾ proposed just such an approach, employing Monte Carlo simulation techniques to accommodate the stochastic nature of the various corrosion processes. They used statistical distributions to describe the effects of variation of the major parameters (impact velocity; particle size; time between successive impacts; materials properties) in the different regimes of erosion identified, and Monte Carlo methods to select discrete impact conditions and to sum the resulting damage. The resulting predictions for erosion-corrosion under simulated gas turbine conditions were very promising, and demonstrated the potential of this approach when the erosion-corrosion process can be described (qualitatively) in mechanistic terms.

What to Recommend for Erosion Resistance?

It appears that the response of metallic materials to low-temperature erosion can, under certain conditions, be described reasonably well by relatively simple models, the parameters of which generally appear to be in accord with intuitive expectations. Nevertheless, where several materials properties are implicated (such as in eqtns. 2 and 3) sometimes the combination of properties necessary for maximizing erosion resistance may not be independently variable, or it may not be apparent that they can be realized in real materials. This may be one of the reasons for the confusion that exists in assessing the erosion resistance of alloys.

There is also a major problem with describing erosion-oxidation behavior because there exists a limited range of conditions under which metallic materials have some chance of application (where the erosive component can damage the oxide scales but not necessarily result in wholesale removal of underlying metal). In such circumstances, it appears that the alloy response depends more on the alloy oxidation properties than on the mechanical properties of the substrate. As a result, the number of variables to be considered and the various caveats

involving the potential interaction of some of these variables lead to confusing signals for engineers looking for practical guidelines for alloy selection.

It appears that the present level of understanding of erosion-corrosion has not been well communicated, or does not lend itself to being communicated to those charged with materials selection in a form that adds to their capabilities. This means that the usual recourse is to rely on practical experience and intuitive expectation, so that selection often is based on materials with increased hardness with some cognizance of the implications of the increased brittleness usually inherent in hard materials. As seen in Fig. 14 (which arbitrarily equates increasing hardness with increasing low-temperature erosion resistance, and increasing engineering reliability with increasing fracture toughness), this course of action leads to the substitution of increasingly harder alloys (using the Stellite series as examples), then to the use of cermets with decreasing levels of binder phase (using the Kennametal WC-Co series). For ultimate hardness ceramic materials are chosen, as suggested in Fig. 14. However, as has been shown by numerous studies, even for ceramics hardness alone is a poor predictor of erosion resistance, and other factors such as microstructure and manufacturing route also have important influences.

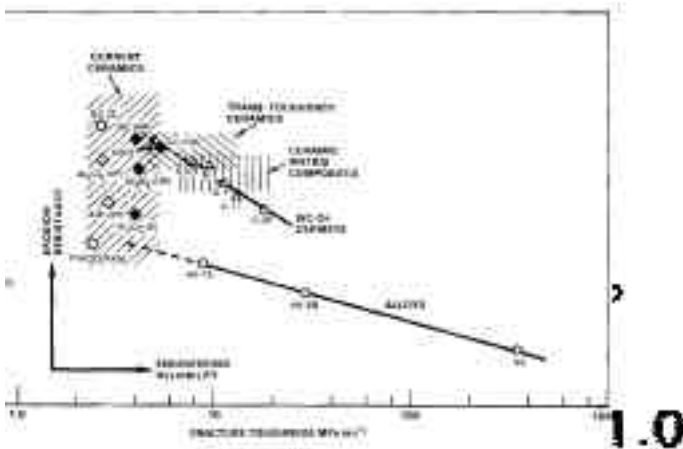


Figure 14. Schematic representation of ranges of 'erosion resistance' and 'engineering reliability' possible with various classes of materials: alloys, cermets, and ceramics⁽³⁶⁾

Practical Guidelines

Practical experience of materials performance under conditions of erosion-oxidation has led to some guidelines for improved performance that have been applied over the years with varying degrees of success. Some of these guidelines are:

1. Reduce the severity of the erosive conditions. This is the solution that addresses the real root cause of the problem. The most obvious action is to reduce the gas and/or solids velocity and the concentration of erodents in the gas stream,

as well as the size of the erodent particles. However, since the erosive conditions can often be very localized, the solution often is to reduce the local velocity and solids loading in the gas stream by evening out the solids velocity and/or distribution across the whole gas stream. This approach is practiced in the convection passes of some coal-fired boilers where mesh screens are used to modify the resistance to gas flow in selected locations. A further way of achieving the same end is to modify the process that gives rise to the erosive gas stream to remove or reduce the loading of solids.

2. Shielding the component from the erodent flow can sometimes be effective. Where a physical shield is used in a hot gas stream, this can often run hotter than the component being protected. The higher metal temperature may be beneficial in that a thicker, more protective surface oxide can be formed, or detrimental if accelerated oxide formation simply translates into accelerated oxide removal by the erodent stream. For flow in pipes, a blocked-tee arrangement often can effectively reduce material loss at pipe bends. In this case a pipe bend is replaced by a T-junction, and the leg of the T not involved in the bend is capped off so that it fills with erodent particles. These then form the surface into which the particles entrained in the fluid stream impact.
3. A widely-used approach is simply to use a thicker component section or to apply a nominally protective (usually harder) coating. These are both sacrificial methods, since the rate of material loss in most cases is not abated. The main aim of these approaches is to increase the time until the component is thinned to a critical thickness so that the components will survive from one scheduled maintenance period to the next.
4. The intuitive response is to use a harder material, as discussed earlier. For the range of hardnesses possible in metallic materials that can be fabricated into components or made into coatings, a factor of approximately three times improvement in life may be possible, at best (c.f. Fig. 14). Where a metallic material is replaced by a cermet, or a ceramic, the subject component typically will require redesigning to compensate for the property differences between the metallic and cermet or ceramic, and so allow the potential advantage to be realized. However, in many cases the need is to replace a component that failed prematurely, so that often there is limited freedom to modify the design of the component, or to modify the environment. In addition, even though cermets and ceramics can be significantly harder than metallic materials, environmental effects still may dominate the erosion oxidation process due to, for instance, preferential oxidation of sintering aids that typically are found at inter-particle boundaries, which then allow removal of individual ceramic particles.

Continuing Issues

Despite the availability of some practically tried remedies and extensive research, one glaring example (among several) of our inability to predict materials behavior under erosion-oxidation conditions is the wastage of heat exchanger tubes immersed in the bed of fluidized-bed combustors. Figure 15 shows data⁽³⁷⁾ for the temperature dependence of metal wastage in a coal-fired fluidized-bed combustor. The temperature

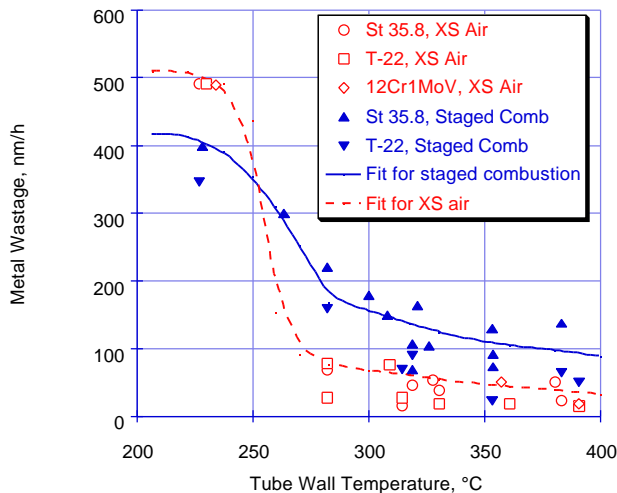


Figure 15. Temperature dependence of tube wastage in an atmospheric pressure FBC, after Tossaint, et al.⁽³⁷⁾

dependence of wastage observed is peculiar and unlike those determined in most laboratory erosion-corrosion rigs. It might be thought to be attributable to the formation of the protective oxide scale, except that the transition to low wastage rates occurs at a temperature far too low for such a protective scale to be formed. In addition, the observation of very similar behavior for alloys containing 2 and 12% chromium does not readily fit this explanation. Such a temperature dependence of wastage has not been reported for fluidized beds with a more vigorous mechanical motion, such as circulating fluidized beds, and experience would suggest that a point is reached where any protective scale or film would be removed by the bed motion.

Although many attempts have been made to reproduce the type of metal wastage observed in fluidized-bed combustors, in terms of the wear pattern developed on in-bed tubes, as well as the temperature dependence of wastage, the type of temperature dependence of metal loss usually observed in a laboratory jet rig is represented in Fig. 16⁽³⁸⁾. Only one laboratory rig has been able to reproduce the former, and show the possibility of reproducing the latter⁽³⁹⁾. This rig used a rod or tube specimen oriented horizontally with respect to the fluidized bed, and had the capability of inducing vertical oscillations in the specimen to better reproduce the relative motion of the specimen and the erodent (bed material). Essentially, it was necessary to resort to mimicking the motion of the real fluidized

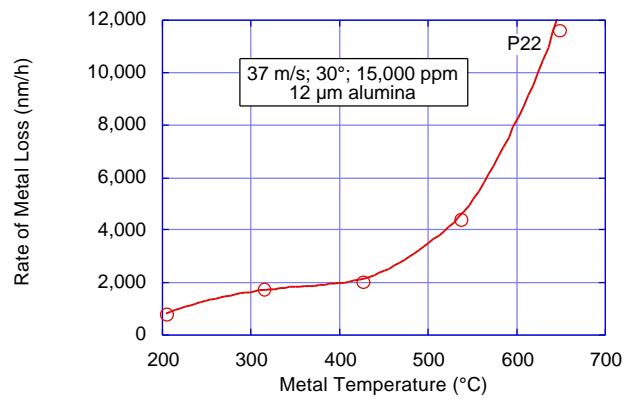


Figure 16. Typical temperature-dependence of erosion-oxidation from laboratory jet-impingement test⁽³⁸⁾.

bed rather than making use of tightly defined conditions of particle flow.

This illustrates important considerations for erosion-oxidation, which are that any simulation testing must be specifically designed for the environment in question, hence the value and relevance of any test data based on simple or standardized testing is questionable. This latter point is illustrated by the examples shown in Table II, which compares the critical measures of the erosive nature of an environment for some typical technologies where erosion-oxidation is a problem. The combination of parameters typical for a laboratory jet rig, which is simply a well-controlled grid blasting apparatus, do not correspond well with any of the combinations for the technologies listed.

Table II. Comparison of Range of Magnitude of Major Parameters Important in Determining the Extent of Erosion in Selected Technologies

Technology	Particle velocity	Angle of impact	Particle loading	d_p
Ash transport pipelines	low	all	high	high
Coal liquefaction processing	high	low	high	low
Pulverized coal-fired boilers	low	all	low	all
Fluidized-bed combustors	low	all	high	high
Gas turbines	high	low	low	low
Grit blasting	high	all	high	all

Summary

Overall, it appears that we know quite a lot about erosion alone, but somewhat less about erosion-oxidation. The very extensive modeling efforts that have been made have pointed out the major materials properties (or combinations) that are important in governing the response of a metallic substrate to erosion and erosion-oxidation, but optimization of these variables is practically difficult since many can be interdependent and the magnitude of the changes possible in the properties of interest may be quite limited. There exist effective

practical measures, often based on a systems approach, for dealing with problems of erosion and erosion-oxidation and these have been listed. The usual approach is to base such measures on prior experience under similar situations and, in the absence of direct data, to resort to comparative testing. However it is cautioned that any testing should use close simulation of the intended application. Standardized erosion tests based on simplified conditions really have limited value. This simply results from the very large number of variables involved and the fact that it is difficult to design an accelerated test without changing the erosion or erosion-oxidation regime. For erosion-oxidation, for instance, the usual route for accelerating erosive attack by increasing the erodent velocity or particle loading can cause a drastic shift in the mechanism of material loss. A useful precaution for any comparative testing is to include a specimen of a standard material in each test run to guard against inadvertent changes in the test conditions. Further, there are still some erosion-corrosion phenomena that we cannot explain, a prime example being the temperature dependence of metal wastage in fluidized-bed combustors.

So, to return to the original question addressed in this paper, is there any reason to continue erosion-corrosion research? To this, the answer must be 'No', if there is an expectation that minor alloying modifications will lead to a large improvement in general resistance to erosion-oxidation. Similarly, the answer should be 'No' where the conditions to be overcome involve very high temperatures, or high particle kinetic energies. However, where a specific microstructure can be shown to offer useful advantages, such as through transformation toughening, or where second-phase particles provide effective shielding at low angles of attack, then further research could be justified. Further, where an improvement in performance of a factor of two or three would make a significant difference, then experimental measurements could be considered worthwhile as long as the key conditions of the intended application were accurately simulated. In addition, further research could be justified if gaining an understanding of specific effects, such as the effect of temperature on a particular material, would allow the operating conditions (environment) of a given process to be adjusted to significantly improve service lifetime or, conversely, would allow some understanding of the potential effects of changes in a specific environment.

Acknowledgements

The author is indebted to numerous colleagues who were responsible for much of the mechanistic research on erosion, and on erosion-corrosion, that provides the underpinning of our current understanding. A particular debt of gratitude is owed to co-researchers who participated in the authors' own work: Drs. A. J. Markworth, V. Nagarajan, V. K. Sethi, and D. K. Shetty, all formerly of Battelle-Columbus. Finally, the contributions of Dr. J. Stringer of EPRI must be acknowledged; he not only funded much of the erosion-corrosion work, but also provided the withering comment and constructive criticism required to provide the perspective that this paper tried to capture.

References

1. I. Finnie, *Wear*, **3**, 87 (1960).
2. I. Finnie, A. Levy and D. H. McFadden, *ASTM Spec. Publ. No. 664* (1979).
3. W. F. Adler, Ed., *Erosion: Prevention and Useful Applications*, ASTM STP-664 (1979).
4. W. F. Adler, "Assessment of the state of knowledge pertaining to solid particle erosion," Report No. CR-79-680 to U. S. Army Research Office (1979).
5. G. P. Tilly, "Erosion caused by impact of solid particles," in *Treaties on Materials Science and Technology, Vol. 13: Wear*, Ed. D. Scott, Academic Press (1979).
6. A. W. Ruff and S. M. Wiederhorn, "Erosion by solid particle impact," in *Treaties on Materials Science and Technology, Vol. 16: Erosion*, Ed. C. M. Preece, Academic Press (1979).
7. I. M. Hutchings, "Mechanisms of the erosion of metals by solid particles," pp. 59-76 in *Erosion: Prevention and Useful Applications*, W. F. Adler, Ed., ASTM STP-664 (1979).
8. P. G. Shewman and G. Sundararajan, "The Erosion of Metals," pp. 301-318 in *Annual Review of Material Science*, R. A. Huggins, Ed., Annual Reviews Inc., Palo Alto (1983).
9. G. P. Tilly and W. Sage, *Wear*, **16**, 447 (1970).
10. G. L. Sheldon and I. Finnie, *Trans. ASME*, **88B**, 387-392 (1966).
11. J. E. Goodwin, W. Sage, and G. P. Tilly, *Proc. Inst. Mech. Engrs. (London)*, **184**, 279 (1969-70).
12. C. E. Smeltzer, M. E. Gulden, S. S. McElmurry and W. A. Compton, "Mechanisms of Sand and Dust Erosion in Gas Turbines," Final Report on Contract DAAJ02-68-C-0056 to U. S. AVLABS, 1970.
13. R. E. Winter and I. M. Hutchings, *Wear*, **29**, 181 (1974).
14. P. V. Rao and D. H. Buckley, *J. Eng. for Gas Turbines and Power*, **107**, 669-678 (1985).
15. I. G. Wright, V. Nagarajan, and J. Stringer, unpublished work, EPRI Contract No. RP-979-8, Battelle-Columbus, 1984.
16. I. Finnie and Y. H. Kabil, *Wear*, **8**, 60 (1965).
17. I. Finnie, J. Wolak and Y. Kabil, *J. Materials*, **2**, 682-700 (1967).
18. M. M. Krushchov, "Resistance of Metals to Wear by Abrasion as Related to Hardness," *Proc. 1957 Conf. on Friction and Wear, Inst. Mech. Eng., London*, p 655 (1957).
19. J. G. A. Bitter, *Wear*, **6**, 5, and 169 (1963).
20. J. H. Neilson and A. Gilchrist, *Wear*, **11**, 111 (1968).
21. G. P. Tilly, *Wear*, **23**, 87 (1973).
22. I. Finnie and D. H. McFadden, *Wear*, **48**, 181-190 (1978).
23. I. M. Hutchings, *Wear*, **70**, 269 (1981).
24. I. M. Hutchings, R. E. Winter, and J. E. Field, *Proc. Royal Soc., London A*, **348**, 379-392 (1976).
25. M. M. Mamoun, Various reports from Argonne National Laboratory to ERDA, Contract W-31-109-Eng-38, especially the Fourth and Fifth Quarterly Reports for periods ending October 15, 1975, and December, 1975.

26. G. Sundararajan and P. G. Shewman, *Wear*, 84, 236-259 (1983).
27. I. G. Wright, V. Nagarajan, and R. B. Herchenroeder, "Some Factors Affecting Solid Particle Erosion/Corrosion of Metals and Alloys," pp. 268-312 in *Corrosion-Erosion Behavior of Materials*, K. Natesan, Ed., TMS-AIME Conference Proceedings (1978).
28. I. G. Wright, V. Nagarajan, and J. Stringer, *Oxidation of Metals*, 25, 175 (1986).
29. V. K. Sethi and I. G. Wright, "Observations on the erosion-oxidation behavior of alloys," pp. 245-264 in *Proc. TMS Conf. On Corrosion and Particle Erosion*, V. Srinivasan and K. Vedula, Eds. (1986).
30. V. K. Sethi and I. G. Wright, "A description of erosion-oxidation based on scale removal and scale erosion," Paper No. 18 in *Proc. Corrosion-Erosion-Wear of Materials at Elevated Temperatures*, A. V. Levy, Ed., NACE, Houston, Texas (1991).
31. G. Sundararajan, *Wear*, 145, 251-282 (1991).
32. I. G. Wright, V. K. Sethi, and A. J. Markworth, unpublished work, Battelle-Columbus (1995).
33. A. J. Markworth, *Mater. Sci. Eng. A*, 150 (1), 37-41 (1992).
34. I. G. Wright, V. K. Sethi, and A. J. Markworth, *Wear*, 186-187, 230-237 (1995).
35. J. R. Nicholls and D. J. Stephenson, *Wear*, 186-187, 64-77 (1995).
36. I. G. Wright, D. K. Shetty, and A. H. Clauer, *J. Materials for Energy Systems*, 6 (3), 172-183 (1984).
37. H. H. J. Tossaint, P. L. F. Rademakers, and P. P. van Norden, paper no. 2.3 in proc. EPRI Workshop on *Wastage of In-Bed Surfaces in Fluidized-Bed Combustion*, EPRI (1987).
38. I. G. Wright, V. Nagarajan, and W. E. Merz, "Erosion-Corrosion of Metals and Alloys at High Temperatures," EPRI Report No. CS-3504 (1984).
39. S. S. MacAdam and J. Stringer, "Temperature-dependence of steel wastage in a bubbling, fluidized-bed simulator," paper No. 141, presented at NACE Corrosion/92, NACE, Houston, Texas (1992).